

1.2.2.- The concept of spring-magnet

In general, it is difficult to obtain large values of coercivity and energy product simultaneously. Actually, hard magnetic materials, with large H_C , usually do not have as large M_S as soft magnetic materials. To overcome this difficulty, Kneller and Hawig proposed in 1991 the concept of *spring-magnet* [16]. The idea was to generate a two-phase microstructure consisting of a small proportion of soft magnetic phase embedded in a hard magnetic matrix, in such a way that both phases became strongly exchange coupled. When performing the hysteresis loop, the magnetization reverses first in the soft phase and then the domain walls propagate from the soft to the hard magnetic phase. The overall magnetic anisotropy is reduced due to the soft phase, consequently H_C usually is found to be smaller than the one of the hard phase alone. However, M_R is significantly enhanced due to the exchange interactions at the interfaces between the soft and the hard grains. These exchange interactions force the spins in each grain, especially at the grain boundaries, to remain aligned in the direction of the previous magnetizing field, once the magnetic field is removed, thus enhancing M_R .

Actually, the first nanocomposites consisting of interacting soft and hard magnetic phases were obtained experimentally before the intuitive concept of spring-magnet was conceived, in 1989, by Coehoorn and co-workers who, by means of melt-spinning of $\text{Nd}_4\text{Fe}_{78}\text{B}_{18}$ synthesized a nanocomposite consisting of exchange interacting $\text{Nd}_2\text{Fe}_{14}\text{B}$, Fe_3B and $\alpha\text{-Fe}$ phases [17]. In the following years, different spring-magnets were synthesized using several techniques, such as rapid solidification methods (e.g. melt-spinning or mechanical alloying) or chemical routes [18-20].

There are several factors which limit the magnetic properties of spring-magnets. In particular, both the mean grain size and the grain size distribution have an effect in M_R , M_R/M_S and H_C [21]. Therefore, precise control of the microstructure of the composites is required to optimize their magnetic properties [22].

1.3.- Phenomenology and Fundamentals of Ferromagnetic-Antiferromagnetic Coupling

1.3.1.- FM-AFM exchange anisotropy

We have already discussed two types of magnetic anisotropies in FM materials: magnetocrystalline anisotropy and shape anisotropy, even though other magnetic anisotropies,

such as stress anisotropy (induced by plastic deformation or mechanical tensions) or surface anisotropy may also be present in a FM material.

In 1956 a new type of magnetic anisotropy was discovered in surface oxidized Co particles [23]. This anisotropy, which is due to the interaction between AFM and FM materials (note that CoO is AFM), was denoted as *exchange anisotropy* or *unidirectional anisotropy* [24].

Since its discovery, this phenomenon, which has its origin in the interactions between the interfacial spins of the FM and the AFM, has been widely studied, in fine particles, bulk inhomogeneous materials, FM-AFM thin films, or thin FM films deposited on the top of AFM monocrystals [24]. Moreover, the effects of exchange coupling have been also observed in ferrimagnetic-AFM and ferrimagnetic-FM materials [25,26].

1.3.2.- Phenomenology

Ferromagnetic-antiferromagnetic exchange coupling is typically induced when a material with a certain number of FM-AFM interfaces is cooled, under the presence of a magnetic field, from a temperature T higher than the Néel temperature (usually the condition $T_N < T < T_C$ has to be fulfilled).

The most well-known effect of FM-AFM coupling is a shift of the hysteresis loop, along the field axis, in the opposite direction of the magnetic field applied during the cooling process. The amount of shift, usually designated by H_E , is called *exchange bias field*. Another feature of FM-AFM coupling is a widening of the hysteresis loop, i.e. an increase of H_C , especially when the AFM anisotropy is low. Both effects (loop shift and coercivity enhancement) tend to decrease with temperature, becoming zero at temperatures close to T_N , due to the loss of magnetic ordering in the AFM. Shown in figure 1.5 are typical hysteresis loops of (a) a FM material and (b) a FM material coupled to an AFM.

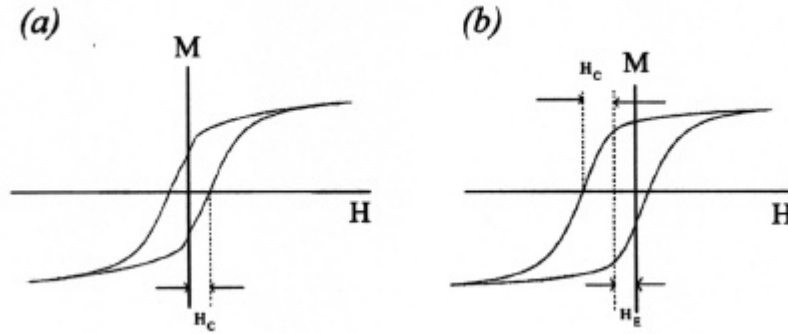


Figure 1.5: Hysteresis loops of (a) a FM material and (b) an exchange coupled FM-AFM material. It can be seen that in (b) the hysteresis loop is shifted along the field axis by an amount H_E and the coercivity, H_C , is enhanced with respect to (a).

Further evidence of FM-AFM coupling can be inferred from torque magnetometry. In torque curves, the force required to rotate the magnetization of a sample out of its easy axis direction is plotted as a function of the angle of rotation [2,4]. For simplicity, let us consider the case of a disc-shaped single crystal with uniaxial anisotropy, i.e. with only one easy axis, and let us assume that the easy axis is in the plane of the disc. If the disc is then suspended in horizontal position and a strong magnetic field is applied, the disc will rotate until its easy axis becomes parallel to the direction of the field. If \mathbf{q} is the angle between the easy axis and the magnetization, M , it can be demonstrated that the anisotropy energy per unit volume will be given by the following expression:

$$E = K_u \sin^2 \mathbf{q} \quad (1.3)$$

where K_u is the anisotropy constant of the uniaxial crystal.

The first derivative of E with respect to \mathbf{q} gives the macroscopic torque, $\mathbf{\Gamma}$, exerted by the external field:

$$\Gamma = -\frac{dE}{d\mathbf{q}} = -2K_u \sin \mathbf{q} \cos \mathbf{q} = -K_u \sin 2\mathbf{q} \quad (1.4)$$

Shown in figure 1.6 (a) are the angular dependences of the energy and torque for a FM material with uniaxial anisotropy. As seen in the figure, there are two positions of minimum energy, for $\mathbf{q} = 0^\circ$ and $\mathbf{q} = 180^\circ$, which are positions of stable equilibrium.

Conversely, in exchange coupled FM-AFM materials, the angular dependence of \mathbf{G} is like the one shown in figure 1.6 (b). In this case, \mathbf{G} can be expressed by the following equation:

$$\mathbf{G} = -K_u \sin \mathbf{q} \quad (1.5)$$

Therefore, the unit volume anisotropy energy is given by:

$$E = K_u \cos \mathbf{q} + E_0 \quad (1.6)$$

where E_0 is an integration constant.

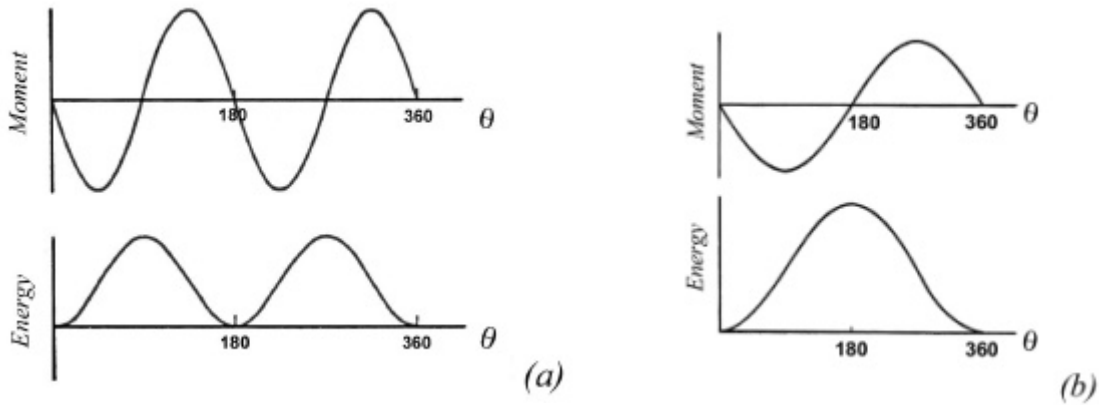


Figure 1.6: Angular dependence of the torque and energy curves in (a) a FM material and (b) an exchange coupled FM-AFM material.

Contrary to the case of an uncoupled FM material, in a FM-AFM couple, there is only one position of minimum energy. In other words, in a FM material with uniaxial anisotropy there are two equivalent equilibrium positions at $\mathbf{q} = 0^\circ$ and $\mathbf{q} = 180^\circ$. However, in a FM-AFM couple only one of these configurations minimizes E , e.g. $\mathbf{q} = 0^\circ$ [23,24]. That is why FM-AFM exchange anisotropy is usually also designated as *unidirectional anisotropy*.

1.3.3.- Intuitive picture

The first model to explain the existence of loop shifts and coercivity enhancements in exchange coupled FM-AFM materials was given by Meiklejohn and Bean in 1956. This model, although it is not able to quantitatively describe all the experimental results reported in

the literature, it gives a good intuitive picture to understand, at least qualitatively, the physical principles of the coupling [23,27].

Shown in figure 1.7 are the spin configurations in the FM and the AFM layers, before and after a field cooling process [24]. If a magnetic field is applied at a temperature T so that $T_N < T < T_C$ and the field is large enough, all the spins in the FM will align parallel to H , i.e. the FM will be saturated. Meanwhile, the spins in the AFM will remain at random, since $T > T_N$. When the FM-AFM couple is cooled through T_N , the magnetic order in the AFM is set up. During the cooling, it is likely that, at the FM-AFM interface, the spins of both components interact with each other. If so, the first layer of spins in the AFM will tend to align parallel to the spins in the FM (assuming ferromagnetic interaction at the interface), while the successive remaining layers in the AFM will orient antiparallel to each other, so as to give a zero net magnetization in the AFM.

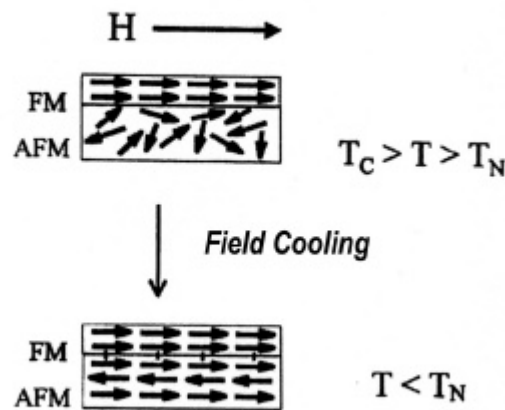


Figure 1.7: Schematic diagram of the spin configurations in a FM-AFM bilayer, before and after a field cooling process.

Within this model, two different opposite cases can be predicted, depending on the AFM magnetic anisotropy. If the AFM anisotropy is low, one should only observe a coercivity enhancement (without any loop shift), while for large AFM anisotropies, the only observed effect should be a shift of the hysteresis loop. Nevertheless, in general, both effects can be observed simultaneously, because, for example, structural defects or grain size distribution bring about local variations of the AFM anisotropy.

The spin configuration, for a FM-AFM couple, is shown schematically in figure 1.8 for different stages of a hysteresis loop [24]. After the field cooling process, the spins in both

the FM and the AFM lie parallel to each other (a). When the magnetic field is reversed, the spins in the FM start to rotate. However, if the AFM anisotropy is large enough, the spins in the AFM will remain fixed. Consequently, due to the coupling, they will exert a microscopic torque to the spins in the FM, trying to keep them in their original position (b). Thus, the magnetic field required to completely reverse the magnetization in the FM will be higher than if the FM was not coupled to an AFM, i.e. an extra magnetic field will be required to overcome the microscopic torque due to the spins in the AFM. And, as a result, the coercivity in the negative field branch increases (c).

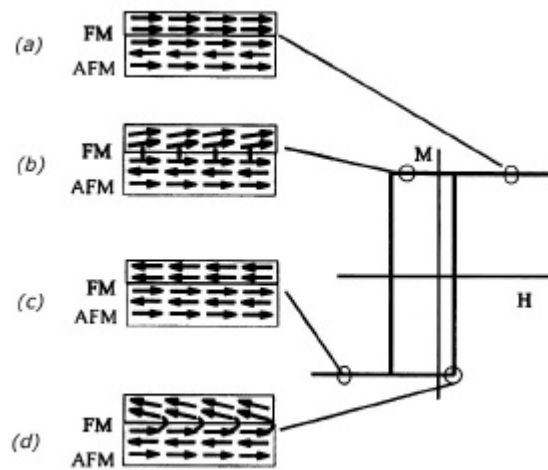


Figure 1.8: Schematic diagram of the spin configurations of a FM-AFM couple at the different stages of a shifted hysteresis loop [24].

Conversely, when the magnetic field is reversed back to positive values, the rotation of spins in the FM will be easier than in an uncoupled FM, since the interaction with the spins in the AFM will favour magnetization reversal, i.e. the AFM will exert a microscopic torque in the same direction as the applied magnetic field (d). Therefore, the coercivity in the positive fields branch will be reduced. The net effect will be a shift of the hysteresis loop along the magnetic field axis. Thus, the spins in the FM have only one stable configuration (unidirectional anisotropy).

When the AFM anisotropy is low the situation is different (see figure 1.9). As in the previous case, after the field cooling, the spins in both layers are aligned in the same direction (a). However, when the magnetic field is reversed and the spins in the FM start to rotate, if the

AFM anisotropy is exceedingly low, the spins in the AFM can be dragged by the spins in the FM (b). In other words, it will be energetically more favourable that the spins in both the FM and the AFM rotate together. However, the AFM spins rotate to a certain angle and finally reach a stable configuration, inducing the necessary irreversibility to induce increased coercivity. An analogous behaviour will be observed after saturating in negative fields ((c) and (d)).

In this case, although no loop shift will be observed, the magnetic field required to reverse magnetizations in both positive and negative branches becomes larger, i.e. an extra energy is required. Consequently, the hysteresis loop widens and the coercivity is enhanced.

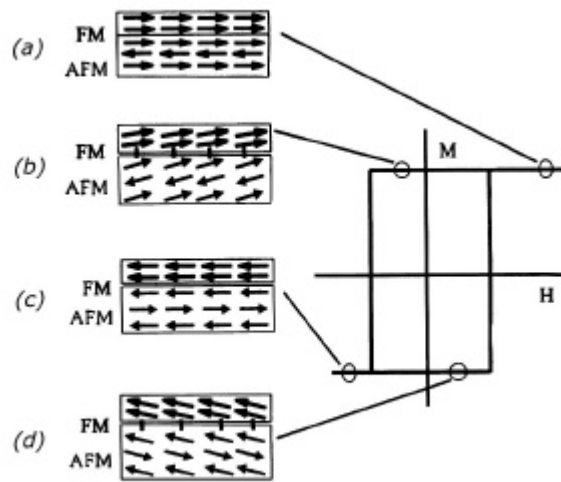


Figure 1.9: Schematic diagram of the spin configurations of a FM-AFM bilayer, at the different stages of a widened hysteresis loop due to the exchange interactions.

Although this phenomenological model gives quite an intuitive and simple image of FM-AFM coupling, it is true that it has serious deficiencies, since it does not consider some key points, such as for example the role of the FM anisotropy in the coupling, the effects of interface roughness, the presence of structural defects or the formation and motion of domain walls.

1.3.4.- Theoretical approach

The model described in the preceding section was the first theoretical approach to exchange bias phenomena. Two of the main assumptions of the model are that the magnetization rotates coherently and the FM and AFM easy axis are parallel. Under these assumptions, the energy per surface unit in the FM-AFM couple can be expressed by [27]:

$$E = -HM_{FM}t_{FM} \cos(\mathbf{q} - \mathbf{b}) + K_{FM}t_{FM} \sin^2(\mathbf{b}) + K_{AFM}t_{AFM} \sin^2(\mathbf{a}) - J_{INT} \cos(\mathbf{b} - \mathbf{a}) \quad (1.7)$$

where H is the applied magnetic field, M_{FM} is the saturation magnetization in the FM, t_{FM} and t_{AFM} are the thicknesses of the FM and AFM layers, K_{FM} and K_{AFM} are the magnetic anisotropies in the FM and the AFM and J_{INT} is the exchange coupling constant at the interface. The angles \mathbf{a} , \mathbf{b} and \mathbf{q} are, respectively, the angles between the planes of spins in the AFM and the AFM easy axis, the direction of the spins in the FM and the FM easy axes and the direction of H and the FM easy axis (see figure 1.10).

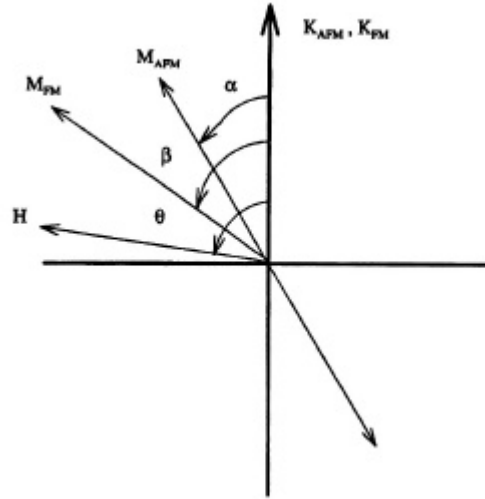


Figure 1.10: Schematic diagram of the angles involved in a FM-AFM exchange coupled system. It is assumed that the easy axes in the FM and AFM layers are collinear.

It can be seen from equation 1.7 that if no coupling exists between the FM and the AFM and the applied magnetic field becomes zero, the overall energy of the FM-AFM system reduces to the terms due to the AFM and the FM magnetic anisotropies (2nd and 3rd terms). However, if a magnetic field is applied, a certain work has to be carried out to rotate the spins in the FM (1st term). Finally, the 4th term represents the FM-AFM coupling. From equation 1.7 one can easily deduce, to first approximation, the value of the exchange bias, H_E , if some assumptions are made. For example, let's first assume that the field is applied along the FM easy axis, i.e. $\mathbf{q} \rightarrow 0$. Secondly, let's suppose that the AFM anisotropy constant is very large, so that the spins of the AFM do not rotate with the field (i.e. they keep aligned along the AFM easy axis, so that $\mathbf{a} \sim 0$ and $\sin^2(\mathbf{a}) \sim 0$). Then eq. 1.7 can be rewritten as follows:

$$E = -HM_{FM}t_{FM} \cos(\mathbf{b}) - J_{INT} \cos(\mathbf{b}) + K_{FM}t_{FM} \sin^2(\mathbf{b}) \quad (1.8a)$$

or reagrouping terms,

$$E = -(HM_{FM}t_{FM} + J_{INT}) \cos(\mathbf{b}) + K_{FM}t_{FM} \sin^2(\mathbf{b}) \quad (1.8b)$$

This equation is analogous to the Stoner-Wohlfarth equation for the energy of single-domain, non-interacting particles, with uniaxial anisotropy, i.e. [3]:

$$E = -(H_{eff}M_{FM}t_{FM}) \cos(\mathbf{b}) + K_{FM}t_{FM} \sin^2(\mathbf{b}) \quad (1.9)$$

Note that equations 1.8(b) and 1.9 are identical if $H_{eff} = H + \frac{J_{INT}}{M_{FM}t_{FM}}$. This indicates that, under these assumptions, the hysteresis loop of the FM-AFM system will be shifted by the amount $H_E = \frac{J_{INT}}{M_{FM}t_{FM}}$ along the magnetic field axis.

Note that, although this formula takes into account some relevant physical parameters of the FM-AFM couple, it assumes, among other factors, a lack of domain structure in the FM and the AFM, co-linearity of the FM and AFM easy axes and absence of structural defects at the interface. Furthermore, it neglects the effect that the magnetic field may have on the spins in the AFM and the possibility of having a completely compensated spin structure in the first layer of spins in the AFM at the interface. Note that a compensated spin structure in the first layer of the AFM means that the spins in this layer are aligned alternatively in opposite directions, so that the net magnetization in the first layer of the AFM is zero.

It is noteworthy that if the magnetic anisotropy in the AFM is low (usually this is expressed by $K_{AFM}t_{AFM} < J_{INT}$) it is energetically more favourable that during the hysteresis loop the spins in the FM and the AFM rotate together, i.e. $(\mathbf{b} - \mathbf{a}) \sim 0$. Then, assuming that H is applied along the FM easy axis, equation 1.7 can be rewritten as follows:

$$E = -HM_{FM}t_{FM} \cos(\mathbf{b}) + K_{FM}t_{FM} \sin^2(\mathbf{b}) + K_{AFM}t_{AFM} \sin^2(\mathbf{b}) - J_{INT} \quad (1.10)$$

Therefore:

$$E = -HM_{FM}t_{FM} \cos(\mathbf{b}) + (K_{FM}t_{FM} + K_{AFM}t_{AFM}) \sin^2(\mathbf{b}) - J_{INT} \quad (1.11)$$

In this case, comparing with equation 1.9, one can observe that $H = H_{eff}$, i.e. there is no loop shift. However, the value of H_C will change, since the overall magnetic anisotropy is modified due to the coupling (see equation 1.1).

Nevertheless, it has to be mentioned that in the framework of Meiklejohn's model it is not possible to predict the observed enhancement of coercivity in exchange interacting FM-AFM couples. Moreover, within this model, choosing appropriate values of the interface exchange constant, J_{INT} , the values predicted for H_E are usually several orders of magnitude larger than the experimental results [28]. Therefore, several authors have developed more complex models, in which many other effects are taken into account. For instance, some models include the effects of the external magnetic field on the AFM [29], the effect of grain size distribution on the FM-AFM coupling [30], the non-collinearity of spins in the FM and AFM layers [31], the spin uncompensation in the AFM [32] or the random anisotropy generated in the AFM, due to the presence of surface roughness at the interface [33] or diluted antiferromagnets [34].

Some models emphasize the importance that the existence of magnetic domains in the AFM can have on the coupling. In this sense, A.P. Malozemoff assumed that, when performing a hysteresis loop of a FM-AFM couple, some domain walls were created in the AFM, perpendicularly to the interface, due to the random fields generated as a consequence of surface roughness or other defects at the interface [33]. According to Malozemoff, the uncompensation of spins due to the AFM magnetic domain structure is mainly responsible for the existence of H_E . Conversely, D. Mauri and N.C. Koon noticed that the formation of domain walls in the AFM, parallel to the interface, could also result in a bias of the hysteresis loop [35]. Furthermore, in Koon's model it was shown that in a completely compensated AFM spin configuration at the interface, the energy is minimized when they are oriented not parallel but perpendicular to the spins in the FM [35]. This is sometimes called *perpendicular coupling*. Nevertheless, T.C. Schulthess and W.H. Butler have recently demonstrated that Koon's model does not actually predict the existence of H_E but only some enhancement of H_C , due to an increase of the uniaxial anisotropy [36]. K. Takano et. al have recently proposed that H_E originates mainly as a consequence of non-compensated interfacial spins in the AFM [32]. They have shown that the temperature dependence of the remanent moment due to the uncompensated spins is similar to the one of H_E , concluding that both effects are closely related to each other. Another approach is the one proposed by M. Kiwi et al., which considers that the effects of the coupling can be explained by an incomplete domain structure

formation in the FM during the field cooling process, basically due to the development of metastable spin configurations at the interface of the FM [37].

Another model by M.D. Stiles and R.D. McMichael takes into account the effects of FM-AFM coupling in polycrystalline FM-AFM bilayers, in which the FM interacts with independent AFM grains (non-interacting) [38]. However, this model has the drawback that it assumes that the crystallite sizes in the AFM are so small that no domain structure can be formed in the AFM.

Moreover, R.E. Camley et al. have performed some numerical simulations, in which, instead of minimizing the overall energy of the FM-AFM couple, they study the temporal evolution of the magnetization during the hysteresis loop [39]. This model predicts a spin structure in the AFM and FM layers similar to that of Koon's model and it shows that the main effect for large K_{AFM} is the existence of H_E , while for low K_{AFM} only an enhancement of H_C should be observed. In addition, this model emphasizes the importance of the applied field direction, with respect to the FM easy axis, in exchange bias and predicts different mechanisms for magnetization reversal, depending on the intensity of the magnetic field. It is noteworthy that different mechanisms of magnetization reversal have been observed also experimentally by several authors [40].

In conclusion, although all these models have succeeded, to some extent, explaining a large variety of experimental results and observations, a complete theory, able to predict all exchange bias related phenomena, is still lacking. This is because usually the models are only applicable to some particular type of materials or cases and cannot be generalized to other systems. Moreover, most models were developed for thin films systems, thus usually can not be exploited to fine particle systems.

1.4.- Ferromagnetic-Antiferromagnetic Coupling in Nanostructures and Fine-Particle Materials

Since the discovery of exchange anisotropy in 1956 in surface-oxidized cobalt fine powders [23], the effects of FM-AFM coupling have been observed in a large variety of different systems [24]. However, since the discovery of spin valves based on exchange bias and its important applications in magnetic storage devices, the bulk of exchange bias research has concentrated in thin film systems [24,41]. Moreover, due to the intrinsic difficulty in controlling several physical parameters, which directly affect the magnitudes of loop shifts and coercivity enhancements, the amount of research in fine particle systems is scarce.

1.4.1.- Exchange bias in fine powders systems

Since their discovery, exchange bias phenomena have been studied in a large number of FM-AFM fine particle systems: Co-CoO [42], Ni-NiO [43], Fe-FeO [44], Fe-Fe₃O₄ [45], Fe-FeS [46], Fe-Fe₂N [47], Co-CoN [48], etc. These particles are usually in the nanometer range (5-100 nm) and typically exhibit a core-shell microstructure, in which a FM inner core is surrounded by an oxide, nitride or sulphide surface layer, obtained either by natural oxidation or chemical treatments of the particles. Several techniques allow the processing of this kind of materials. Among them, vapour deposition, chemical reduction, gas condensation, aerosol spray pyrolysis or mechanical alloying are the most frequently used [24,49].

Although loop shifts have been observed in FM-AFM fine particles, the main characteristic of this type of systems is the enhancement of the coercivity occurring at $T < T_N$. Consequently, exchange bias was suggested as a possible route for permanent magnet processing. However, in fine-particle systems, the properties of exchange bias are only usually observed for temperatures below room temperature. This is in part because many AFM have Néel temperatures below room temperature (e.g. $T_N(\text{FeO}) = 200$ K, $T_N(\text{CoO}) = 290$ K) [24]. In addition, the thin AFM shell (usually only a few nm) and the reduced size of the AFM crystallites also limits the temperature range in which the interactions can occur. When the AFM thickness or grain size becomes increasingly small, thermal fluctuations cause a loss of the AFM magnetic ordering, i.e. they become superparamagnetic. When heating a FM-AFM couple, the temperature at which the effects of the coupling disappear is called the *blocking temperature* and is designated as T_B . It has been found experimentally that T_B is progressively reduced as the AFM grain size or thickness decreases, becoming $T_B \ll T_N$ for AFM crystallite sizes or film thickness of a few nm [50,51]. However, probably the main reason of the limited research in exchange biased particles is that these systems are not ideal for studies of fundamental aspects of exchange bias, since distributions of particle sizes and shapes, often difficult to control, are always present. Moreover, it is very difficult to control some key parameters which play an important role in the FM-AFM coupling, such as AFM or FM layer thicknesses, interface roughness, crystallinity or stoichiometry. Finally, from a technological point of view, the fact that the AFM phases are usually formed or derived from the FM cores represents a severe limitation to the number of systems in which FM-AFM interactions can be induced. For instance, in general, it is difficult to obtain AFM phases by chemically treating the surface of hard magnetic particles.

Additionally, some interest has arisen in *pure* FM, AFM and ferrimagnetic nanoparticles, since sometimes they also exhibit loop shifts and coercivity enhancements [52,53]. These effects are generally attributed to the existence of a spin-glass-like layer surrounding each particle due to surface disorder (e.g. uncoupled spins or roughness). During

a field cooling process, the spin-glass layer can become “frozen” and thus couple to the AFM, FM or ferrimagnetic cores. Note that, due to their random magnetic configuration, spin glasses can play the role of both FM and AFM in FM-AFM coupling [24].

1.4.2.- Exchange bias in “artificially-fabricated” magnetic nanostructures

Recently, some work is also being carried out in artificially fabricated FM-AFM nanostructures. By “artificially-fabricated”, we mean nanostructures grown controllably by different lithography methods. Several types of FM-AFM nanostructures are worth studying or are actually being studied at present (see figure 1.11): (a) oxidized arrays of nanoparticles [54,55], (b) FM-AFM nanoparticles [56-58] or (c) FM nanoparticles on continuous AFM layers. Coercivity enhancements and loop shifts have been observed in these systems, which make them promising candidates to solve some of the miniaturization trends of the recording industry [54-58].

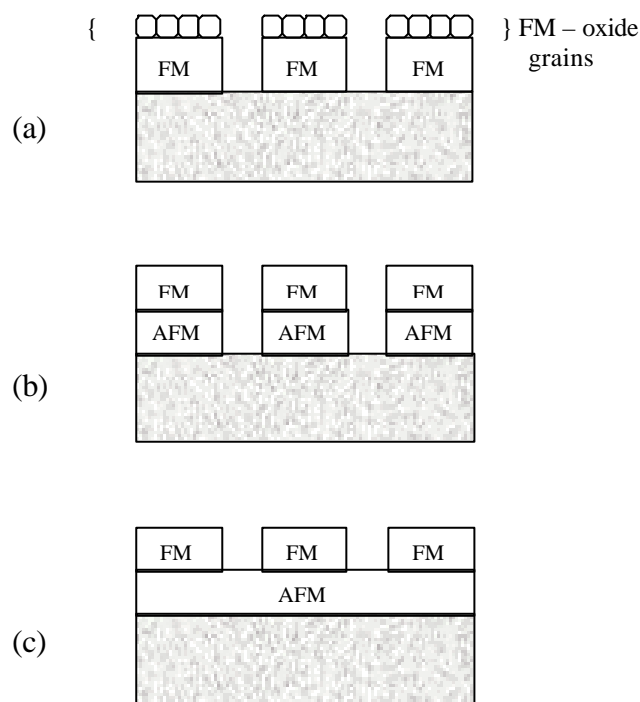


Figure 1.11: Schematic configurations of three different artificially fabricated FM-AFM nanostructures: oxidized arrays of nanoparticles (a), FM-AFM nanoparticles (b) and FM nanoparticles on continuous AFM layers (c).

Although type (a) is similar to random particles, types (b) and (c) solve many of the problems of exchange bias in fine particles, since in these systems many structural parameters can be precisely controlled. Thus, these FM-AFM nanocomposites are ideal systems for theoretical modelling of the exchange bias phenomena since, by controlling the size of the particles (or dots) it is possible, in some cases, to tune the magnetic domain structure in both the FM and the AFM and, thus, corroborate or invalidate some of theoretical predictions on the exchange bias phenomena [54-58]. However, in these patterned elements, some effects due to shape anisotropy or dipolar interactions are also usually present. This requires accurate control of some parameters, such as the separation between dots or the element aspect ratio, in order to isolate the effects of exchange bias from other effects.

References

- [1] Y. Ishikawa, N. Miura, *Physics and Engineering Applications of Magnetism*. (Springer-Verlag, Berlin, 1991).
- [2] S. Chikazumi, *Physics of Magnetism*. (John Wiley & Sons Inc., New York, 1964).
- [3] R. Skomski, J.M.D. Coey, *Permanent Magnetism*. (Institute of Physics Publishing, Bristol and Philadelphia, 1999).
- [4] R.C. O’Handley, *Modern Magnetic Materials, Principles and Applications* (John Wiley & Sons, Inc., New York, 2000).
- [5] A. Hernando, J.M. Rojo, *Física de los Materiales Magnéticos* (Síntesis, DL, Madrid 2001).
- [6] G.C. Hadjipanayis, *J. Magn. Magn. Mater.* **200** (1999) 373.
- [7] A.E. Clark, *Appl. Phys. Lett.* **23** (1973) 642.
- [8] G.C. Hadjipanayis, R.C. Hazelton, K.R. Lawless, *Appl. Phys. Lett.* **43** (1983) 797.
- [9] F.E. Pinkerton, *J. Magn. Magn. Mater.* **54-57** (1986) 579.
- [10] R. Coehoorn, J.P.W.B. Duchateau, C.J.M. Demissen, *J. Appl. Phys.* **65** (1989) 704.
- [11] G.B. Clemente, J.E. Keem, *J. Appl. Phys.* **64** (1988) 5299.
- [12] J. Rivas, M.A. López-Quintela, M.G. Bonome, R.J. Duro, J.M. Greneche, *J. Magn. Magn. Mater.* **122** (1993) 1.
- [13] E.C. Stoner, E.P. Wohlfarth, *Philos. Trans. R. Soc. A* **240** (1948) 599.
- [14] C.P. Bean, J.D. Livingston, *J. Appl. Phys.* **30** (1959) 124S.
- [15] R.W. Chantrell, J. Popplewell, S. W. Charles, *IEEE Trans. Magn.* **14** (1978) 975.
- [16] E.F. Kneller, R. Hawig, *IEEE Trans. Magn.* **27** (1991) 3588.
- [17] R. Coehoorn, D.B. Mooji, C.D. de Waard, *J. Magn. Magn. Mater.* **80** (1989) 101.
- [18] G.C. Hadjipanayis, L. Withanawasam, R.F. Krause, *IEEE Trans. Magn.* **31** (1995) 3596.

- [19] P.G. McCormick, W.F. Miao, P.A.I. Smith, J. Ding, R. Street, *J. Appl. Phys.* **83** (1998) 6256.
- [20] J. Ding, P.G. McCormick, R. Street, *J. Magn. Magn. Mater.* **124** (1993) 1.
- [21] T. Schrefl, R. Fisher, J. Fidler, H. Kronmüller, *J. Appl. Phys.* **76** (1994) 7053.
- [22] K. O'Donnell, C. Kuhrt, J.M.D. Coey, *J. Appl. Phys.* **76** (1994) 7068.
- [23] W.H. Meiklejohn, C.P. Bean, *Phys. Rev.* **102** (1956) 1413; W.H. Meiklejohn, C.P. Bean, *Phys. Rev.* **105** (1957) 904.
- [24] For reviews see: J. Nogués, I.K. Schuller, *J. Magn. Magn. Mater.* **192** (1999) 203; A.E. Berkowitz, K. Takano, *J. Magn. Magn. Mater.* **200** (1999) 552; R. L. Stamps, *J. Phys. D: Appl. Phys.* **33** (2000) R247; M. Kiwi, *J. Magn. Magn. Mater.* **234** (2001) 548.
- [25] P.J. van der Zaag, R.M. Wolf, A.R. Ball, C. Bordel, L.F. Feiner, R. Jungblut, *J. Magn. Magn. Mater.* **148** (1995) 346.
- [26] W.C. Cain, M.H. Kryder, *J. Appl. Phys.* **67** (1990) 5722.
- [27] W. H. Meiklejohn, *J. Appl. Phys.* **33** (1962) 1328.
- [28] R. Jungblut, R. Coehoorn, M.T. Johnson, J. aan de Stegge, A. Reinders, *J. Appl. Phys.* **75** (1994) 6659.
- [29] K.B. Vlasov, A. Mishchek, *Phys. Met. Metall.* **14** (1962) 487.
- [30] S.H. Charap, E. Fulcomer, *J. Appl. Phys.* **42** (1971) 1426; E. Fulcomer, S.H. Charap, *J. Appl. Phys.* **43** (1972) 4190.
- [31] Y.S. Sanoyan, K.A. Yegiyanyan, *Phys. Met. Metall.* **38** (1974) 231.
- [32] K. Takano, R.H. Kodama, A.E. Berkowitz, W. Cao, G. Thomas, *Phys. Rev. Lett.* **79** (1997) 1130.
- [33] A.P. Malozemoff, *Phys. Rev. B* **35** (1987) 3679; A.P. Malozemoff, *Phys. Rev. B* **37** (1988) 7673; A.P. Malozemoff, *J. Appl. Phys.* **63** (1988) 3874.
- [34] P. Miltényi, M. Gierlings, J. Keller, B. Beschoten, G. Güntherodt, U. Nowak, K.D. Usadel, *Phys. Rev. Lett.* **84** (2000) 4224.

- [35] D. Mauri, H.C. Siegmann, P.S. Bagus, E. Kay, *J. Appl. Phys.* **62** (1987) 3047; N.C. Koon, *Phys. Rev. Lett.* **78** (1997) 4865.
- [36] T.C. Schulthess, W.H. Butler, *Phys. Rev. Lett.* **81** (1998) 4516; T.C. Schulthess, W.H. Butler, *J. Magn. Magn. Mater.* **198-199** (1999) 321.
- [37] M. Kiwi, J. Mejía-López, R.D. Portugal, R. Ramírez, *Europhys. Lett.* **48** (1999) 573; M. Kiwi, J. Mejía-López, R.D. Portugal, R. Ramírez, *Appl. Phys. Lett.* **75** (1999) 3995.
- [38] M.D. Stiles, R.D. McMichael, *Phys. Rev. B* **59** (1999) 3722.
- [39] R.E. Camley, B.V. McGath, R.J. Aсталos, *J. Vac. Sci. Technol. A* **17** (1999) 1335.
- [40] V. I. Nikitenko, V.S. Gornakov, L.M. Dedukh, Yu P. Kabanov, A.F. Khapikov, A.J. Shapiro, R.D. Shull, A. Chaiken, R.P. Michil, *Phys. Rev. B* **57** (1998) 57; M.R. Fitzsimmons, P. Yashar, C. Leighton, I.K. Schuller, J. Nogués, C.F. Majkrzak, J.A. Dura, *Phys. Rev. Lett.* **84** (2000) 3986.
- [41] B. Dieny, V. S. Speriosu, S. S. P. Parkin, B. A. Gurney, D. R. Wilhoit, D. Mauri, *Phys. Rev. B* **43** (1991) 1297; B. Dieny, *J. Magn. Magn. Mater.* **136** (1994) 335.
- [42] D. S. Geoghegan, P.G. McCormick, R. Street, *Mater. Sci. Forum* **179-181** (1995) 629; S. Gangopadhyay, G.C. Hadjipanayis, C. M. Sorensen, K.J. Klabunde, *J. Appl. Phys.* **73** (1993) 6964; I.N. Krivorotov, H. Yan, E.D. Dahlberg, A. Stein, *J. Magn. Magn. Mater.* **226-230** (2001) 1800.
- [43] Y. D. Yao, Y. Y. Chen, M.F. Tai, D. H. Wang, H. M. Lin, *Mater. Sci. Eng. A* **217/218** (1996) 281; J. Löffler, W. Wagner, H. Van Swygenhoven, J. Meier, B. Doudin, J. P. Ansermet, *Mater. Sci. Forum* **235-238** (1997) 699; A.J. García-Bastida, R.D. Sánchez, J. García-Otero, J. Rivas, A. González-Penedo, J. Solla, M.A. López-Quintela, *Mat. Sci. Forum* **269-272** (1998) 919.
- [44] W. H. Meiklejohn, *J. Appl. Phys.* **29** (1958) 454.
- [45] V. Papaefthymiou, A. Kostikas, A. Simopulos, D. Niarchos, S. Gangopadhyay, G.C. Hadjipanayis, C.M. Sorensen, K.J. Klabunde, *J. Appl. Phys.* **67** (1990) 4487; Y. Du, J. Wu, H. Lu, T. Wang, Z. Qiu, H. Tang, J. C. Walker, *J. Appl. Phys.* **61** (1987) 3314; M Uotani, T. Taniyama, Y. Yamazaki, *J. Appl. Phys.* **87** (2000) 5585.
- [46] H. Heffner, G. Wade, *J. Appl. Phys.* **31** (1960) 2316; J. H. Greiner, I. M. Croll, M. Sulich, *J. Appl. Phys.* **32** (1961) 188S.
- [47] C. M. Hsu, H. M. Lin, K. R. Tsai, *J. Appl. Phys.* **76** (1994) 4793.

- [48] H. M. Lin, C. M. Hsu, Y. D. Yao, Y. Y. Chen, T. T. Kuan, F. A. Kuan, F. A. Yang, C. Y. Tung, *Nanostruct. Mater.* **6** (1995) 977.
- [49] G. C. Hadjipanayis, Z. X. Tang, S. Gangopadhyay, L. Yiping, C. M. Sorensen, K. J. Klabude, A. Kostikas, V. Papaefthymiou, *Studies of Magnetic Fine Particles and their Relevance to Materials Science*, J. L. Dorman and D. Fiorani (Editors) (Elsevier Science Publishers B.V., 1992), p. 35.
- [50] T. Ambrose, C. L. Chien, *J. Appl. Phys.* **83** (1998) 6822; T. Ambrose, C. L. Chien, *J. Appl. Phys.* **83** (1998) 7222.
- [51] S. Soeya, T. Imagawa, K. Mitsuoka, S. Narishige, *J. Appl. Phys.* **76** (1994) 5356; P. J. van der Zaag, A. R. Ball, L. F. Feiner, R. M. Wolf, P. A. A. van der Heijden, *J. Appl. Phys.* **79** (1996) 5103; J. Fujikata, K. Hayashi, H. Yamamoto, M. Nakada, *J. Appl. Phys.* **83** (1998) 7210.
- [52] R. H. Kodama, A. E. Berkowitz, E. J. McNiff, S. Foner, *Phys. Rev. Lett.* **77** (1996) 394; R. H. Kodama, S. A. Makhlof, A. E. Berkowitz, *Phys. Rev. Lett.* **79** (1997) 1393.
- [53] G. F. Goya, H. R. Rechenberg, J. Z. Jiang, *Mater. Sci. Forum* **312-314** (1999) 545; B. Martínez, T. Obradors, Ll. Balcells, A. Rounanet, C. Monty, *Phys. Rev. Lett.* **80** (1998) 181; Y. Shi, J. Ding, *J. Appl. Phys.* **90** (2001) 4078.
- [54] A. S. Ross, R. Chantrell, M. Hwang, M. Farhoud, T. A. Savas, Y. Hao, H. Smith, F. M. Ross, M. Redjal, F. B. Humphrey, *Phys. Rev. B* **62** (2000) 14252; C. A. Ross, M. Farhoud, M. Hwang, H. I. Smith, M. Redjal, F. B. Humphrey, *J. Appl. Phys.* **89** (2001) 1310.
- [55] M. Rutnakornpituk, M. S. Thompson, L. A. Harris, K. E. Farmer, A. R. Esker, J. S. Riffle, J. Connolly, T. G. St. Pierre, *Polymer* **43** (2002) 2337.
- [56] L. Sun, Y. Ding, C. L. Chien, P. C. Searson, *Phys. Rev. B* **64** (2001) 184430; J. Yu, A. D. Kent, S. S. P. Parkin, *J. Appl. Phys.* **87** (2000) 5049; S. Mao, J. Giusti, N. Amin, J. Van ek, Ed Murdock, *J. Appl. Phys.* **85** (1999) 6112.
- [57] K. Liu, S. M. Baker, M. Tuominen, T. P. Russell, I. K. Schuller, *Phys. Rev. B* **63** (2001) 060403; R.E. Dudin-Borkowski, M.R. McCartney, B. Cardinal, M.R. Scheinfein, D. J. Smith, S. S. P. Parkin, *J. Appl. Phys.* **90** (2001) 2899.
- [58] S. Landis, B. Rodmacq, B. Dieny, B. Dal'Zotto, S. Tedesco, M. Heitzman, *Appl. Phys. Lett.* **75** (1999) 2473; M. Fraune, U. Rüdiger, G. Güntherodt, S. Cardoso, P. Freitas, *Appl. Phys. Lett.* **77** (2000) 3815.